



# Influence of Al<sub>2</sub>O<sub>3</sub> nanoreinforcement on the adhesion and thermomechanical properties for epoxy adhesive

Nur Zalikha Khalil<sup>a,\*</sup>, Mohamed Feisal Johanne<sup>b</sup>, Mahadzir Ishak<sup>a</sup>

<sup>a</sup> Manufacturing Focus Group, Faculty of Mechanical and Manufacturing Engineering, Universiti Malaysia Pahang, 26600 Pekan, Pahang, Malaysia

<sup>b</sup> Faculty of Mechanical and Manufacturing Engineering, Universiti Malaysia Pahang, 26600 Pekan, Pahang, Malaysia

## ARTICLE INFO

### Keywords:

Polymer-matrix composites (PMCs)  
Wettability  
Mechanical properties  
Fracture

## ABSTRACT

In present work, an attempt was made to investigate the effect of alumina nanoparticle (ANP) reinforcement to the wetting and mechanical properties of adhesively bonded aluminum alloy with epoxy adhesive. ANP of 13 nm size in 0–2 wt% concentration was utilized to be incorporated into two components epoxy adhesive to evaluate its effect on wetting behaviour and tensile shear strength. The addition of ANP results in improved contact angle and spreading area of the adhesive. The inclusion of ANP content up to 1.0 wt% demonstrates approximately 54.2% improvement of tensile shear stress as compared to its pristine epoxy counterpart. In this work, it is observed that regardless of ANP concentration, fractured specimens demonstrate the combination of both adhesive and cohesive fracture (CF) region, with highest CF region observed at 1.0 wt% ANP reinforcement. From thermomechanical analysis results, at 30 °C significant increment of both storage and loss modulus up to 68.3% and 17.3% respectively is achieved with 0.5 wt% ANP inclusion.

## 1. Introduction

In recent years, adhesive joining technique has emerged as an attractive alternative due to its advantages like having prospect of manufacturing low cost components, high strength to weight ratio and more uniform stress distribution. Moreover, adhesive joining has a relatively easier and fewer processing requirements when compared to conventional joining technique such as mechanical fastening and welding [1,2]. For instance, in comparison to welding technique which often require post weld treatments to relieve residual stress and to obtain specific mechanical properties, adhesive joining on the other hand generally require little or no post process treatment. These advantages have in fact enabled adhesive joining to find its applications in many industrial fields, such as automobiles, medical appliances, electronics, and aeronautics sectors. However, there is an issue for adopting adhesive joining as primary joining medium. This include its poor mechanical performance, associated with the presence of stress concentration at free edges on the bonding area, resulting in premature failure at the adherend it joints [3,4]. Essentially, there are some available methods for reducing the stress concentration. These include joint end geometry modification, adherend shaping, forming adhesive fillet and hybrid double lap. Nevertheless, these techniques suffer in terms of

manufacturing difficulty due to geometry complexity, leading to cost-inefficiency for industrial applications [3]. To tackle the above-mentioned issue, researchers have proposed to incorporate nano-fillers into structural adhesive. It is acknowledged that nano-reinforcement provide the flexibility for polymeric material to be tailored with desired properties for specific applications [5,6]. The inclusion of nano-filler into polymeric adhesive is anticipated to enhance stress transfer between the filler and polymer matrix, resulting in improved strength of the joining components [3,4,7–9]. The existence of nano-fillers was also suggested to facilitate easier penetration into small voids or irregularities on the adherend surface and thus improving the joint strength by mechanical interlocking. In particular, nanoparticle was proposed to introduce mechanical keying of the nanoadhesive into the irregularities on the adherend surface, leading to the intrinsic adhesion, thus resulting in higher mechanical strength in the joining components [10,11]. To date, considerable efforts [1–9] have been devoted to assess the viability of nano-filler inclusion to improve bonding performance. For instance, Tutunchini et al. [4] has reported that the addition up to 3 wt% TiO<sub>2</sub> content into acrylic adhesive has resulted in significant improvement in both tensile and shear strength, while further addition beyond that concentration will only deter the bonding performance. In earlier work on carbon nanofiller (CNF), Vietri

\* Corresponding author.

E-mail addresses: [nurzalikhak@ump.edu.my](mailto:nurzalikhak@ump.edu.my), [daisyrose87@yahoo.com](mailto:daisyrose87@yahoo.com) (N.Z. Khalil).

<https://doi.org/10.1016/j.compositesb.2019.05.007>

Received 9 September 2018; Received in revised form 22 February 2019; Accepted 5 May 2019

Available online 6 May 2019

1359-8368/© 2019 Elsevier Ltd. All rights reserved.

et al. [2] has reported that 1.3 wt% CNF to be the most relevant concentration to be added into epoxy adhesive in order to improve mechanical properties of the joining, in which further addition of CNF will only lead to adverse effect in the joining performance. Similar trend was also observed by Chavooshian et al. [9] when working with silicon carbide nanoparticle (SNP) reinforced into two components acrylic adhesive. The mechanical performance of the joining was reported to only show significant enhancement up to 1.5 wt% content of SNP before showing a deterioration after exceeding that concentration.

It appears that regardless of the type of nanoparticles, improvement of mechanical performance for the joining can only be achieved with specific nanoparticles concentration inclusion, in which further addition beyond certain concentration will hamper bonding performance. While it is apparent that the effect of nano reinforcement to joining performance follows a specific trend, there are however, limited reports which assess the reinforcement effect to the fracture behavior of the adhesive bonding, and the relation between these two elements is not well understood [9,12]. With an aim to provide better understanding of the aforementioned concern, present work has been carried out to investigate the effect of nano reinforcement to the adhesion properties of the joining, and subsequently characterize the resultant failure behavior of the adherend it joints. An attempt has also been made to correlate the effect of the reinforcement to the wetting behavior, bonding performance and the fracture behavior of the joining to obtain a thorough understanding on the effect of nanoparticle inclusion into these three factors. In present study, various concentration of ANP is employed into structural epoxy adhesive to joint aluminum alloy. Wetting behavior of the nano-reinforced adhesive was investigated by measuring the spread area and contact angle while the mechanical performance of the joining was evaluated using tensile shear test. Microstructural analysis of the fracture surface is performed to assess the failure mode in the joint specimen. Finally, thermomechanical analysis utilizing dynamic mechanical analysis was also carried out to characterize the viscoelastic response of the nanoreinforced epoxy adhesive.

2. Experimental procedures

2.1. Materials

In present work, commercially available ANP with particle size of 13 nm supplied by Sigma Aldrich was utilized as the nano-filler. Fig. 1 illustrates the morphology of as received ANP in both low and high magnifications. A commercially available Pioneer all-purpose adhesive 1:1 two component epoxies adhesive (viscosity 800,000 cps at 25 °C, cures at 8 h) supplied by Republic Chemical Industries, Inc (Quezon City, Philippines) was used to bond 1100-O pure aluminum alloy plates (adherend). The chemical composition for the AA1100 Aluminum alloy is illustrated in Table 1.

2.2. Preparation of adherend and nanoadhesive

The aluminum alloy adherend was first pre-cleaned using ethanol to remove existing contaminants on the adherend surface before subjected to abrasive powder blasting for 60 s at a pressure of 621 kPa. This is followed by degreasing with ethanol to remove remaining debris and lastly dry blown using compressed air. This pretreatment process is also intended to add surface roughness of the adherend prior to joining process. In present work, preparation of nano adhesives was done in three steps to increase homogeneous dispersion of ANP in the epoxy solution. The highly viscose adhesive component (part A) was first diluted in ethanol solution using magnetic stirrer in 2: 1 vol ratio for about 5 min at 1000 rpm before adding different amount of ANP (0,0.5,1,1.5 and 2 wt%) into the solution. Each adhesive solution containing different ANP concentration was continuously stirred by magnetic and mechanical stirring for about 1 h at 3000 rpm until the all the ethanol has evaporated. Lastly, the hardener (part B) was added to the

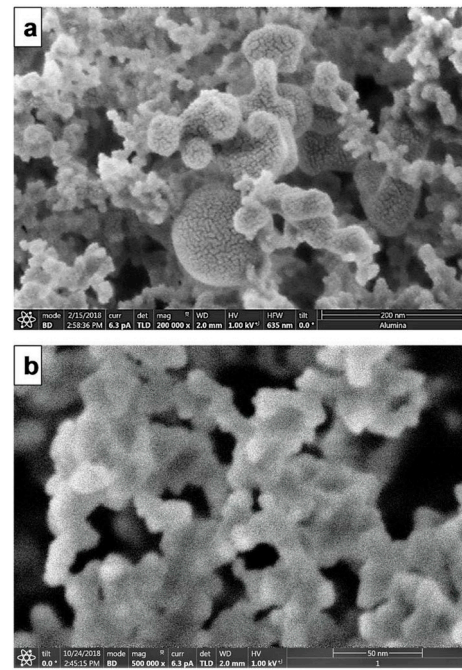


Fig. 1. SEM micrographs of as received ANP in (a) low and (b) high magnification.

Table 1  
Chemical composition of AA1100-O adherend.

Element	Fe	Si	Mg	Mn	Cu	Zn	Ti	Al
Mass (%)	0.35	0.25	0.01	0.01	0.05	0.01	0.02	Balance

solution in 1:1 vol ratio and mechanically stirred for about 1 min before applying a thin layer onto the surface of the adherend. The joints were clamped together by exerting 1 kg weight for 24 h to ensure a uniform bond line thickness (approximately 0.8 mm) is achieved. The joint geometry was prepared according to the existing international standard practice for single lap joint specimen (ASTM D 1002) as shown in Fig. 2. Additional holes were made at the grip area of the specimen to enable the positioning to a customized jig made for tensile shear test purpose.

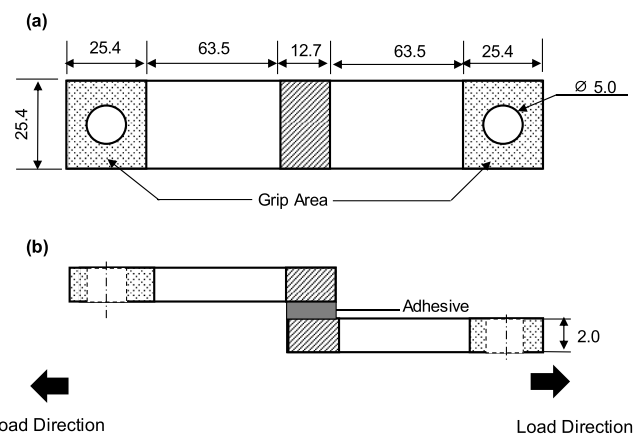


Fig. 2. Schematic of the tensile shear test for single lap joint specimen (a) dimension in mm according to ASTM D 1002; (b) schematic of single lap joint specimen (load direction).

2.3. Characterization

2.3.1. Tensile shear test

The adhesion strength of the single lap joint specimens was evaluated using tensile test machine with a crosshead speed of 1.3 mm/min using Universal Instron tensile test machine, 50 kN load. A customized slotted jig was used to accommodate the geometric dimension of the single lap joint specimen. For each ANP concentration, at least five sets of joint specimens were tested at room temperature to obtain an average value.

2.3.2. Wettability measurement

Wetting behavior of nano reinforced adhesive was evaluated by contact angle and spread area measurement. For this purpose, 2 mL volume of nano reinforced epoxy adhesive drop was deposited onto the pretreated adherend surface and the drop images were taken (after 1 min) using a smartphone attached with macro lens, when the droplet images appear the sharpest and clearest. The measurement setup is shown in Fig. 3. The images taken were then analyzed by using ImageJ software and the calculation of the contact angle of the droplet was performed by applying spherical approximation technique [13,14]. A total of five measurements for each ANP concentration were taken to obtain an average value.

2.3.3. Thermomechanical analysis

Thermomechanical properties of the ANP reinforced adhesive was conducted by using DMA analysis under DMA 8000 (Perkin-Elmer) with dual cantilever bending mode at a frequency of 1 Hz with temperature scan. Rectangular specimens of 3 mm (T) × 5 mm (W) × 50 mm (L) were used for the analysis. The analysis was carried out in a heating rate of 2 °C/min with operating temperature range from 30 °C to 180 °C.

3. Results and discussions

3.1. Wetting behavior

Fig. 4 illustrates the representative images of spreading area and contact angle of nanoreinforced adhesive with different content of ANP. A total of five measurements for both spread area and contact angle were taken to obtain the average value. Fig. 5 summarizes the relation between spreading area, *A* and contact angle,  $\theta$  as a function of ANP concentration. Essentially, spreading area and contact angle are among


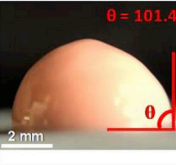

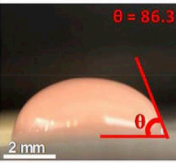
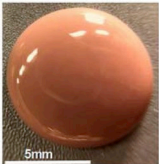
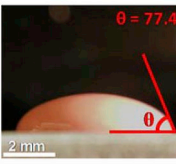
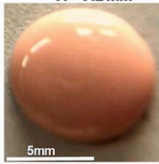
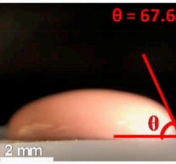

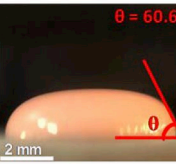
	Spreading Area, <i>A</i>	Contact Angle, $\theta$
0 wt%	<i>A</i> = 2.7 mm <sup>2</sup> 	$\theta$ = 101.4° 
0.5 wt%	<i>A</i> = 5.1 mm <sup>2</sup> 	$\theta$ = 86.3° 
1.0 wt%	<i>A</i> = 5.5 mm <sup>2</sup> 	$\theta$ = 77.4° 
1.5 wt%	<i>A</i> = 7.2 mm <sup>2</sup> 	$\theta$ = 67.6° 
2.0 wt%	<i>A</i> = 10.8 mm <sup>2</sup> 	$\theta$ = 60.6° 

Fig. 4. Representative of spreading area and contact angle for nanoreinforced adhesive droplet with different ANP concentration.

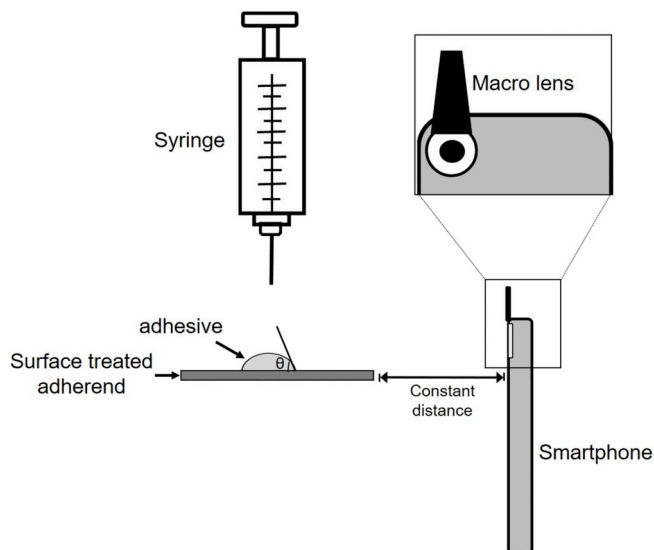


Fig. 3. Contact angle measurement setup using smartphone attached with macro lens.

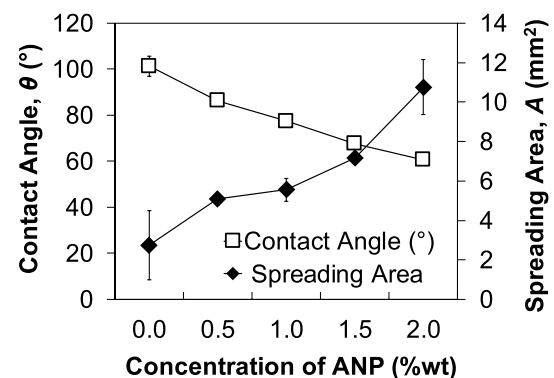


Fig. 5. Spreading area, *A* and contact angle,  $\theta$  as a function of ANP concentration.

common parameters used to indicate the wettability of a surface material in such that, smaller contact angle and/or larger spreading area represents larger wetting tendency of a particular material [15]. Apparently, with the increment of ANP concentrations, the spreading area of the reinforced adhesive demonstrates an increment, while a decrease for contact angle is observed, suggesting that the wetting ability of the nano adhesive is increasing. Possible explanation for this observation might be inferred to the higher difference in surface and interface free energy for nanoparticle, due to higher surface free energy

in the nanoparticle [16]. As a result, the adhesive become more hydrophilic, hence improving its wettability [4,17].

### 3.2. Mechanical properties

Fig. 6(a) illustrates the representative nominal stress-nominal strain curves for the adhesively joint Al alloy having different ANP concentration. Fig. 6 (b)-(c) summarize the relation between stresses and elongations as a function of ANP concentration. Apparently, it is observed that with 1.0 wt% ANP concentration, both shear stress and stress at break show significant improvement up to 54.2% and 91.7% respectively as compared to its pristine adhesive counterpart. Further increment exceeding 1.0 wt% ANP concentration leads to deterioration of joining strength. It is previously proposed that the size of nanofiller in polymer composite govern the surface to volume ratio of the fillers, in such that the ratio represents the quantity of interfacial region [18]. In the context of present work, it may be proposed that the addition of ANP up to 1.0 wt % concentration in the epoxy adhesive has resulted in higher surface to volume ratio of ANP, increasing the quantity of interfacial region, and thus improving the stress distribution/transfer leading to a higher bonding performance. The effect may have been further pronounced by the mechanical interlocking effect between ANP with the existent irregularities and pores on the adherend surface, leading to improvement in the interfacial adhesion [11]. On earlier finding by Meguid et al. [19] with their work on alumina nanoparticle and epoxy/carbon fiber laminates, it was reported that when nanoparticle content exceeds a certain amount the amount of porosity/pores on the adherend become relatively smaller in which additional number of nanoparticle could no longer fill the porosity/pores on the adherend

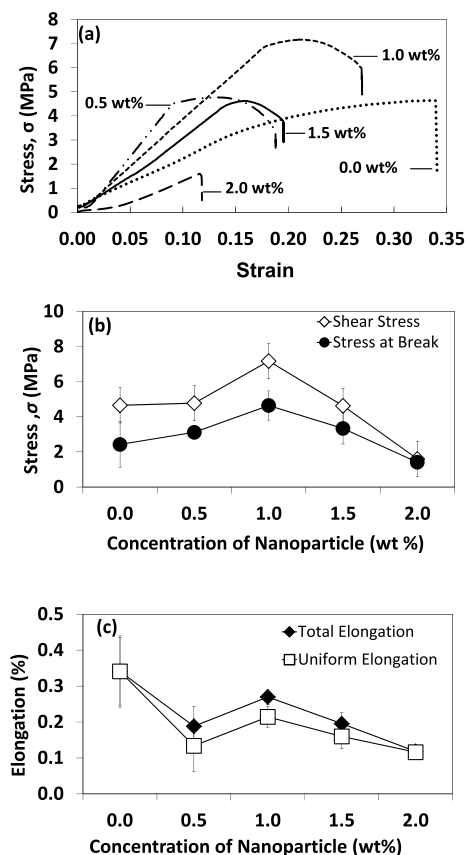


Fig. 6. Tensile properties of nanoreinforced adhesive at different ANP concentration (a) Representative nominal stress-nominal strain, (b) and (c) illustrate the correlation between ANP concentration with stress and elongations (total and uniform) respectively.

to induce mechanical interlocking mechanism. This in turn leads to infectivity interaction within the polymer matrix combined with poor matrix infiltration. As a result, the polymer molecule is forced to adapt to a strained form, modifying the initial structure of the polymer causing it to be easily deboned.

From Fig. 6(c), it is observed that the pristine epoxy adhesive shows the largest elongations at approximately 0.34% and subsequent addition of ANP content up to 0.5 wt% demonstrates a decreasing trend in the elongations. However, further ANP inclusion up to 1.0 wt% content is observed to increase both total and uniform elongation before again decreases when the ANP content exceeds 1.0 wt%. With this regard, possible justification may be inferred to the mobility reduction of the polymeric chains as nanoparticle content increases, leading to easier debonding behavior [20]. As the content of nanoparticle exceeds 0.5 wt %, it may be proposed that the toughening effect induced by further addition of nanoparticles overcome the negative influence causes by the polymer chain reduction, resulting in an increase for both total and uniform elongation [9]. Subsequent addition of nanoparticle concentration exceeding 1.0 wt% may have resulted to nanoparticles segregation, and consequently hamper the elongations. To summarize, in present work the inclusion of 1.0 wt% of ANP concentration is found to be the relevant content to improve joining performance, in which further addition beyond that concentration deteriorate the bonding performance. The strength of nanoreinforced adhesive might be affected by few possible factors, in such that the effective strength for the adhesive is a result of interplay between several potential strengthening/toughening mechanisms as discussed above. With regard to present work, it is beneficial in the future to undertake detailed and systematic investigations elucidate the underlying mechanism affecting the bonding performance of nanoadhesive.

### 3.3. Fracture behavior

Failure modes in adhesive joining are conveniently classified into 2 modes; namely adhesive fracture (AF) and cohesive fracture (CF). AF refers to the failure which occurs between the adhesive layer and one of the adherends, also known as interfacial failure. CF on the other hand, refers to a failure caused by separation in such a manner that both adherend surfaces remained covered with adhesive [21]. From Fig. 7, it is apparent that regardless of ANP concentration, all the joint specimens exhibit a combination of AF and CF (red colored regions refer to CFed region). The identification of cohesive and adhesive fractured region was done by color contrast of the fractured specimen's image. To analyze the trend of the failure behavior, the surface area of each failure mode is divided by the overlap surface area to obtain failure mode ratio for each specimen condition. For each ANP concentration, at least a total of 3 specimens were utilized to obtain an average value. The failure modes ratio of the specimen for each ANP concentration is presented in the parenthesis. Fig. 8 summarizes the dependency for fracture mode ratios (adhesive fracture,  $A_F$  and cohesive fracture  $A_C$ ) of single lap joint specimens as a function of nanoparticle concentration,  $C$ . It can be observed that the variation of ANP concentration leads to 2 distinct trends in the fracture modes ratio. The relation between ANP content with failure modes ratio is found to best fit quadratic relation as shown in the Fig. 8. As the content of ANP increases, it can be seen that the AF mode ratio first decrease before increases when ANP content exceeds 1.0 wt% (Fig. 8 a). On the contrary, the increment of ANP content shows the increment of CF mode up to 1.0 wt % before decreasing after exceeding that concentration. It is generally acknowledged that CF mode within the adhesive is the ideal failure type as this serve as an indicator that the maximum strength of the joint materials is reached [21]. In present work, the highest CF mode in the fractured specimen is observed when the ANP content reach 1.0 wt %. It is also noted that, the trend corresponds with tensile shear test result as discussed in section 3.2, in which joining performance with 1.0 wt% ANP content is observed to demonstrate highest shear strength. Possible justification for these

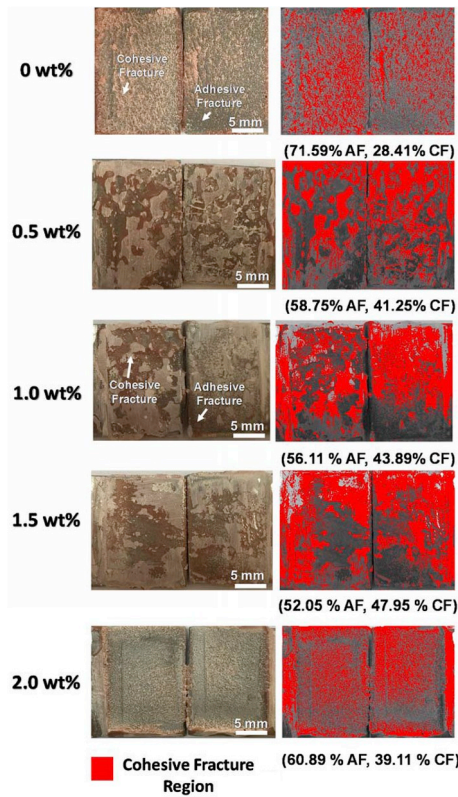


Fig. 7. Representative of fracture surface of single lap joint specimens showing the existence of both AF and CF modes regardless of ANP concentration. Red colored regions indicate the cohesive fractured region. (For interpretation of the references to color in this figure legend, the reader is referred to the Web version of this article.)

observations might be inferred to the higher energy required to cause debonding in the joining, and thus higher shear stress [22,23]. However, detailed investigations are needed to identify the exact mechanism. As a summary, within the ANP content investigated, regardless of ANP content, it is observed that all fractured specimens demonstrate a combination of AF and CF modes. The trend of each fracture mode is best fit with quadratic relation in such that CF mode ratio is observed to the highest in the sample with 1.0 wt% ANP.

### 3.4. Thermomechanical properties

Fig. 9 and Fig. 10 illustrate the storage modulus and loss modulus result for the ANP reinforced epoxy adhesive respectively. These viscoelastic moduli are also known as complex modulus measure the resistance of viscoelastic material to deformation, including both the elastic and viscous responses [24]. Storage modulus essentially measures the recoverable stored strain energy or the “stiffness” of the material while loss modulus measures of the energy dissipated generally lost as heat [24,25]. These temperature dependent moduli are especially important for structural analysis when considering stiffness-based design [26]. In this work, it is observed that the addition of ANP up to 0.5 wt% results in two distinct trends in the modulus value when compared to its pristine adhesive counterpart. In specific, at lower temperature range (30 °C –60 °C) both storage and loss modulus exhibit higher values while at higher temperature range (90 °C –120 °C), modulus value exhibit slight increment/retention (Figs. 9 b, Fig 10 b). Meanwhile, further addition exceeding 0.5 wt % ANP results in the decrement in the value of these moduli regardless of the temperature range. It is also noted that 0.5 wt % ANP inclusion at 30 °C demonstrate highest value of both storage and loss modulus with approximately

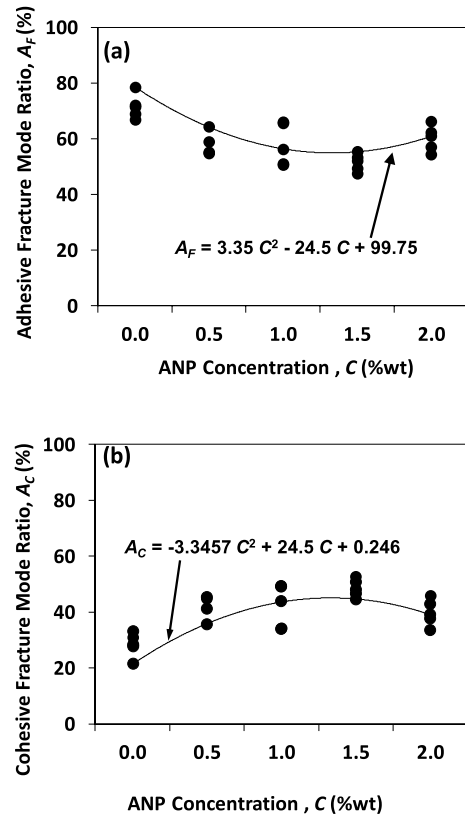


Fig. 8. Scatter plot graph illustrating the trend of (a) adhesive and (b) cohesive failure mode ratio in the single lap joint specimen.

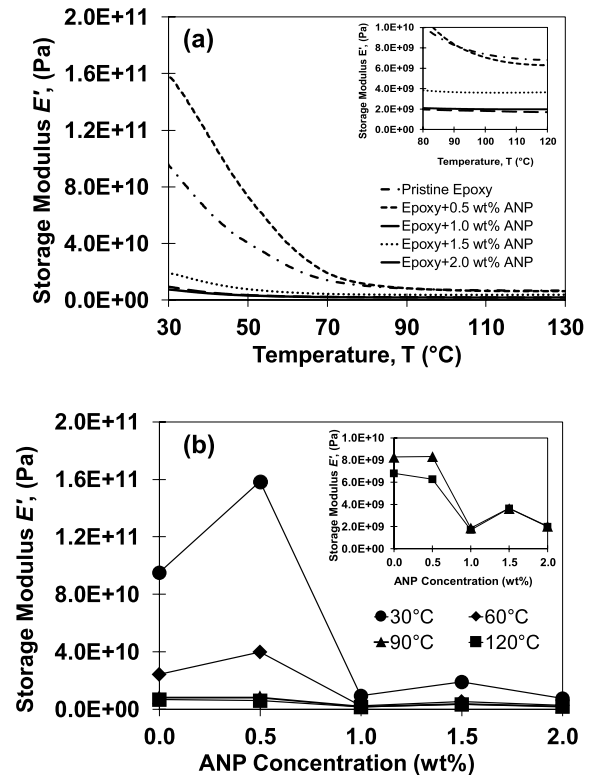


Fig. 9. Storage modulus for ANP reinforced epoxy adhesive (a) as a function of temperature in the 30–130 °C temperature range (b) as a function of ANP weight percent at different temperature.

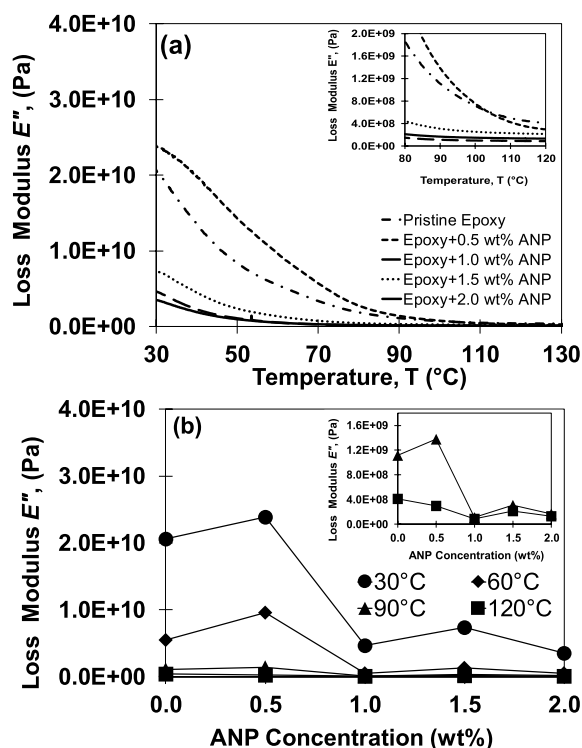


Fig. 10. Loss modulus for ANP reinforced epoxy adhesive (a) as a function of temperature in the 30–130 °C temperature range (b) as a function of ANP weight percent at different temperature.

68.3% and 17.3% increment respectively as compared to pristine epoxy adhesive counterpart. In earlier work, it was suggested that the higher value of complex modulus with nanoparticle addition may be inferred to the improvement of the stiffness of epoxy adhesive due to the physical interaction between nanoparticle and polymer matrix, restricting the mobility of the polymer chains in the vicinity of nanoreinforcement [25]. At higher nanoparticle content, the increasing tendency of nanoparticle to agglomerate might attribute to easier motion of polymeric chain resulting in decrease in the modulus values [27]. Moreover, it is also proposed that higher temperature may cause free movement of the polymer chains leading to lower values for these moduli [25]. Similar findings were reported in several earlier works [27,28]. It appears that complex modulus of ANP reinforced epoxy adhesive might be affected by several factors (i.e. content of ANP and temperature) in such that the effective value of both moduli might be the result of interplay between several potential mechanism as discussed above. A detailed and systematic study are required to elucidate the exact mechanism involved.

#### 4. Conclusions

This work has investigated the effect of ANP reinforcement to the adhesion and thermomechanical properties two components structural epoxy adhesive and the following conclusions can be drawn;

1. The inclusion of ANP has resulted in the increment of spreading area and decrease in contact angle of the nano reinforced adhesive, which imply the improvement of wetting behavior.
2. In the range ANP content investigated, the inclusion of ANP up to 1.0 wt% content has resulted in significant improvement of tensile shear strength up to 54% as compared to its pristine epoxy counterpart. Further addition exceeding the ANP concentration leads to decrease in tensile shear strength.
3. Regardless of ANP content, the fracture modes in the fractured specimens demonstrate a combination of both AF and CF mode. The

dependency of ANP concentration on the fracture behavior is found to best represented by quadratic relation. The CF mode area is demonstrated to be the highest when the ANP content reach 1.0 wt%, showing good complement with the result from tensile shear test.

4. The addition of ANP up to 0.5 wt% results in two distinct trends in the complex modulus value. At lower temperature range (30 °C –60 °C), both storage and loss modulus demonstrate higher values, while at higher temperature range (90 °C –120 °C), modulus value show slight increment/retention. Further addition exceeding 0.5 wt % ANP content results in the decrement in the value of complex modulus regardless of the temperature range. 0.5 wt % ANP inclusion at 30 °C demonstrate highest value of both modulus with approximately 68.3% and 17.3% increment respectively as compared to pristine epoxy adhesive counterpart

#### Acknowledgments

This work was funded by Universiti Malaysia Pahang (UMP) provided under the grant RDU 1703309. The financial support is gratefully acknowledged.

#### Appendix A. Supplementary data

Supplementary data to this article can be found online at <https://doi.org/10.1016/j.compositesb.2019.05.007>.

#### References

- [1] Hsiao K-T, Alms J, Advani SG. Use of epoxy/multiwalled carbon nanotubes as adhesives to join graphite fibre reinforced polymer composites. *Nanotechnology* 2003;14:791–3. <https://doi.org/10.1088/0957-4484/14/7/316>.
- [2] Vietri U, Guadagno L, Raimondo M, Vertuccio L, Lafdi K. Nanofilled epoxy adhesive for structural aeronautic materials. *Compos B Eng* 2014;61:73–83. <https://doi.org/10.1016/J.COMPOSITESB.2014.01.032>.
- [3] Carbas RJC, da Silva LFM, Andrés LFS. Functionally graded adhesive joints by graded mixing of nanoparticles. *Int J Adhes Adhes* 2017;76:30–7. <https://doi.org/10.1016/J.IJADH.2017.02.004>.
- [4] Tutunchi A, Kamali R, Kianvash A. Adhesive strength of steel–epoxy composite joints bonded with structural acrylic adhesives filled with silica nanoparticles. *J Adhes Sci Technol* 2015;29:195–206. <https://doi.org/10.1080/01694243.2014.981469>.
- [5] Zhang Y, Heo Y-J, Son Y-R, In I, An K-H, Kim B-J, et al. Recent advanced thermal interfacial materials: a review of conducting mechanisms and parameters of carbon materials. *Carbon N Y* 2019;142:445–60. <https://doi.org/10.1016/J.CARBON.2018.10.077>.
- [6] Zhang Y, Rhee KY, Hui D, Park S-J. A critical review of nanodiamond based nanocomposites: synthesis, properties and applications. *Compos B Eng* 2018;143:19–27. <https://doi.org/10.1016/J.COMPOSITESB.2018.01.028>.
- [7] Ascione F. The influence of adhesion defects on the collapse of FRP adhesive joints. *Compos B Eng* 2016;87:291–8. <https://doi.org/10.1016/J.COMPOSITESB.2015.10.033>.
- [8] Akpınar S. The strength of the adhesively bonded step-lap joints for different step numbers. *Compos B Eng* 2014;67:170–8. <https://doi.org/10.1016/J.COMPOSITESB.2014.06.023>.
- [9] Chavooshian M, Kamali R, Tutunchi A, Kianvash A. Effect of silicon carbide nanoparticles on the adhesion strength of steel–epoxy composite joints bonded with acrylic adhesives. *J Adhes Sci Technol* 2017;31:345–57. <https://doi.org/10.1080/01694243.2016.1215015>.
- [10] Allen KW. Acrylates as reactive adhesives. *Int J Adhes Adhes* 1989;9:103–5. [https://doi.org/10.1016/0143-7496\(89\)90032-8](https://doi.org/10.1016/0143-7496(89)90032-8).
- [11] Shi D, He P, Wang SX, Ooi J WJ van, Wang LM, Zhao J, et al. Interfacial particle bonding via an ultrathin polymer film on Al<sub>2</sub>O<sub>3</sub> nanoparticles by plasma polymerization. *J Mater Res* 2002;17:981–90. <https://doi.org/10.1557/JMR.2002.0146>.
- [12] Budhe S, Banea MD, de Barros S, da Silva LFM. An updated review of adhesively bonded joints in composite materials. *Int J Adhes Adhes* 2017;72:30–42. <https://doi.org/10.1016/J.IJADH.2016.10.010>.
- [13] Prydatko AV, Belyaeva LA, Jiang L, Lima LMC, Schneider GF. Contact angle measurement of free-standing square-millimeter single-layer graphene. *Nat Commun* 2018;9:4185. <https://doi.org/10.1038/s41467-018-06608-0>.
- [14] ImageJ -Image processing and Analysis in Java n.d. <https://imagej.nih.gov/ij/index.html> (accessed December 3, 2018).
- [15] Dwivedi C, Pandey I, Pandey H, Ramteke PW, Pandey AC, Mishra SB, et al. Chapter 9 electrospun nanofibrous Scaffold as a potential carrier of antimicrobial therapeutics for diabetic wound healing and tissue regeneration. 2018. p. 147–64. <https://doi.org/10.1016/b978-0-323-52727-9.00009-1>.

- [16] Chen X, You B, Zhou S, Wu L. Surface and interface characterization of polyester-based polyurethane/nano-silica composites. *Surf Interface Anal* 2003;35:369–74. <https://doi.org/10.1002/sia.1544>.
- [17] Lim S, Horiuchi H, Nikolov AD, Wasan D. Nanofluids alter the surface wettability of solids. *Langmuir* 2015;31:5827–35. <https://doi.org/10.1021/acs.langmuir.5b00799>.
- [18] Crosby AJ, Lee J. Polymer nanocomposites: the “nano” effect on mechanical properties. *Polym Rev* 2007;47:217–29. <https://doi.org/10.1080/15583720701271278>.
- [19] Meguid S, Sun Y. On the tensile and shear strength of nano-reinforced composite interfaces. *Mater Des* 2004;25:289–96. <https://doi.org/10.1016/J.MATDES.2003.10.018>.
- [20] Shah D, Maiti P, Jiang DD, Batt CA, Giannelis EP. Effect of nanoparticle mobility on toughness of polymer nanocomposites. *Adv Mater* 2005;17:525–8. <https://doi.org/10.1002/adma.200400984>.
- [21] Introduction and adhesion theories. *Handb Adhes Surf Prep* 2011:3–13. <https://doi.org/10.1016/B978-1-4377-4461-3.10001-X>.
- [22] Tutunchi A, Kamali R, Kianvash A. Effect of Al<sub>2</sub>O<sub>3</sub> nanoparticles on the steel-glass/epoxy composite joint bonded by a two-component structural acrylic adhesive. *Soft Mater* 2016;14:1–8. <https://doi.org/10.1080/1539445X.2014.1003269>.
- [23] Dorigato A, Pegoretti A. The role of alumina nanoparticles in epoxy adhesives. *J Nanoparticle Res* 2011. <https://doi.org/10.1007/s11051-010-0130-0>.
- [24] Modification and Engineering of HSREP to Achieve Unique Properties. *Elastomeric polym with high rate sensit*. 2015. p. 319–45. <https://doi.org/10.1016/B978-0-323-35400-4.00009-X>.
- [25] Saba N, Jawaid M, Alothman OY, Paridah MT. A review on dynamic mechanical properties of natural fibre reinforced polymer composites. *Constr Build Mater* 2016;106:149–59. <https://doi.org/10.1016/J.CONBUILDMAT.2015.12.075>.
- [26] de Souza JPB, dos Reis JML. A thermomechanical and adhesion analysis of epoxy/Al<sub>2</sub>O<sub>3</sub> nanocomposites. *Nanomater Nanotechnol* 2015;5:18. <https://doi.org/10.5772/60938>.
- [27] Kumar K, Ghosh PK, Kumar A. Improving mechanical and thermal properties of TiO<sub>2</sub>-epoxy nanocomposite. *Compos B Eng* 2016;97:353–60. <https://doi.org/10.1016/J.COMPOSITESB.2016.04.080>.
- [28] Chen C-H, Jian J-Y, Yen F-S. Preparation and characterization of epoxy/ $\gamma$ -aluminum oxide nanocomposites. *Compos Part A Appl Sci Manuf* 2009;40:463–8. <https://doi.org/10.1016/J.COMPOSITESA.2009.01.010>.